Chapter 1
A morpho-elastic model of hyphal tip growth in filamentous organisms.

Alain Goriely, Michael Tabor, and Anthony Tongen

1.1 Introduction

The growth of filamentous cells such as fungi, actinomycetes, root hairs, and pollen tubes has been a long-standing topic of interest to microbiologists. Although there are many fundamental differences in the structure, life cycles, size, and function of these diverse cells, the overall pattern of growth appears to share certain fundamental features: most notably that the hyphal growth is apical, *i.e.* the growth and incorporation of new cell wall material is concentrated at the tip of the cell. The fact that such diverse cell types grow with this general morphology suggests, at the mechanical level of description, a fairly universal process reflecting a growth driven interplay between the anisotropy of the cell wall and the mechanical stresses. Space does not permit a comprehensive review of the the associated biological and mathematical literature, and we refer the reader to a number of articles in the field [1, 2, 3, 4].

1.2 Nonlinear elastic models of hyphal growth

Our approach to modeling hyphal growth is that of *morpho-elasticity*, namely a process of continuous growth and a corresponding elastic response to that growth.

A. Goriely
Program in Applied Mathematics and Department of Mathematics, University of Arizona, Building #89, Tucson, AZ 85721 e-mail: goriely@math.arizona.edu

M. Tabor
Program in Applied Mathematics and Department of Mathematics, University of Arizona, Building #89, Tucson, AZ 85721 e-mail: tabor@math.arizona.edu

A. Tongen
Department of Mathematics, James Madison University, Harrisonburg, VA 22807

The model described here represents a generalization of our earlier work on this topic [5, 6].

The hyphal wall is represented as an axi-symmetric elastic shell whose basic geometry is shown in Figure 1.1. The shape, which is assumed to be rotationally symmetric about the z-axis, is described in terms of the variables $(s(\sigma), r(\sigma))$,which represent, respectively, the arc-length distance of a material point σ from the tip and the distance of the point from the z-axis. A deformation of an initial shape $(\sigma, \rho(\sigma))$ is described in terms of of the deformation variables

$$\alpha_s = \frac{ds}{d\sigma}, \qquad \alpha_\varphi = \frac{r(\sigma)}{\rho(\sigma)}. \tag{1.1}$$

The variables α_s and α_φ measure, respectively, the meridional and azimuthal

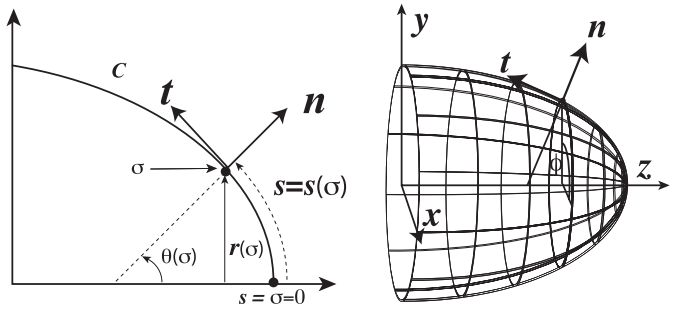

Fig. 1.1 Basic hyphal geometry. A material point σ is measured by its arc-length, $s(\sigma)$ from the apex of the shell and its position $r(\sigma)$ on a curve C, **n** and **t** denotes the normal and tangent vectors at that point. The angle $\theta(s)$ is the angle between the normal direction. The hyphal wall is taken to be axisymmetric where φ is the azimuthal angle.

stretches of the shell. For an incompressible shell the third deformation variable, α_3, measuring changes in the normal thickness of the shell, is simply related to α_s and α_φ through the incompressibility condition $\alpha_s\alpha_\varphi\alpha_3 = 1$. The geometric variables satisfy the equations $dr/ds = \cos(\theta), dz/ds = \sin(\theta)$, and the principal curvatures of the shell are given by $\kappa_s = d\theta/ds, \kappa_\varphi = (\sin\theta)/r$.

The mechanical equilibrium, including bending moments, is governed by the equations [7]

$$\frac{1}{r}\frac{d(rq_s)}{ds} = q_n - \left(\kappa_s t_s + \kappa_\varphi t_\varphi\right), \tag{1.2}$$

$$\frac{1}{r}\frac{d(rt_s)}{ds} = \frac{\cos\theta}{r}t_\varphi + \kappa_s q_s - \tau_s, \tag{1.3}$$

$$\frac{1}{r}\frac{d(rm_s)}{ds} = \frac{\cos\theta}{r}m_\varphi + q_s, \tag{1.4}$$

where t_s and t_φ are, respectively, the meridional and azimuthal stresses; m_s and m_φ are the bending moments; and q_s is the shear stress normal to the surface. In

equation (1.2), which represents the balance of normal stresses, q_n represents the total normal stress exerted on the shell, e.g. If the problem is pressure driven then $q_n = \Delta P$, namely the pressure difference (turgor) across the shell. τ_s is the external tangential shear stress acting on the shell which can be used here to represent the friction between the growing hypha and its environment.

In order to close the system of mechanical and geometric equations constitutive relations must be introduced. These are developed through the introduction of an elastic free energy function, specified as energy per unit volume, $W = W(I_1, I_2, I_3)$, where I_1, I_2, I_3 are the strain invariants $I_1 = \alpha_s^2 + \alpha_\varphi^2 + \alpha_3^2, I_2 = \alpha_s^2\alpha_\varphi^2 + \alpha_s^2\alpha_3^2 + \alpha_\varphi^2\alpha_3^2, I_3 = \alpha_s\alpha_\varphi\alpha_3$. The incompressibility condition implies that both $\alpha_3 = 1/\alpha_s\alpha_\varphi$ and that W does not depend on the third strain invariant, $I_3 = 1$. One can then show that the stresses are given by the relations

$$t_s = 2h\alpha_3(\alpha_s^2 - \alpha_3^2)\left(\frac{\partial W}{\partial I_1} + \alpha_\varphi^2\frac{\partial W}{\partial I_2}\right), \quad t_\varphi = 2h\alpha_3(\alpha_\varphi^2 - \alpha_3^2)\left(\frac{\partial W}{\partial I_1} + \alpha_s^2\frac{\partial W}{\partial I_2}\right) \tag{1.5}$$

where h is the shell thickness, and the factor $h\alpha_3$ represents the change in wall thickness in the current (*i.e.* stressed) configuration [8].

The choice of W depends on the problem at hand. A popular choice for elastomers is the Mooney-Rivlin model $W_{\rm mr} = C_1(I_1 - 3) + C_2(I_2 - 3)$, where C_1 and C_2 are certain elastic parameters. When $C_2 = 0$, $W_{\rm mr}$ reduces to the neo-Hookean model, and for small deformation C_1 is related to Young's modulus, E, by $E = 6C_1$. We note that despite its linearity in the invariants the Mooney-Rivlin potential, and its neo-Hookean limit, is still capable of describing finite, *i.e.* nonlinear, deformations. Given any model, we write the constitutive relationships in the form $t_s = Af_s(\alpha_s, \alpha_\varphi), \quad t_\varphi = Af_\varphi(\alpha_s, \alpha_\varphi)$, where f_s, f_ϕ are dimensionless functions and A provides the dimensional factor appropriate for the scaling of the equilibrium equations. For the neo-Hookean and Mooney-Rivlin energies $A = 2C_1h = Eh/3$. Finally, we need to specify a constitutive relationships for the bending moments. The bending moments are assumed to be isotropic and proportional to the change in the surface's mean curvature, *i.e.* $m_\varphi = m_s = B(\kappa_s + \kappa_\varphi - K_0)$, where K_0 is the initial mean curvature and B is the bending modulus [7].

The geometric and mechanical equations can be combined to give a closed system. It is convenient to express all the derivatives in terms of the material coordinate, σ, leading to

$$\frac{dz}{d\sigma} = \alpha_s\sin(\theta), \quad \frac{dr}{d\sigma} = \alpha_s\cos(\theta), \quad \frac{d\theta}{d\sigma} = \alpha_s\kappa_s, \tag{1.6}$$

$$\frac{d\kappa_s}{d\sigma} = \alpha_s\left[\frac{\cos\theta}{r}\left(\frac{\sin\theta}{r} - \kappa_s\right) + \frac{q_s}{B}\right], \tag{1.7}$$

$$\frac{dt_s}{ds} = \alpha_s A\left[\frac{\cos\theta}{r}(f_\varphi - f_s) + \kappa_s\frac{q_s}{A} - \frac{\tau_s}{A}\right], \tag{1.8}$$

$$\frac{dq_s}{d\sigma} = \alpha_s A\left[\frac{q_n}{A} - \kappa_s f_s - \frac{\sin\theta}{r} f_\varphi - \frac{q_s}{A}\frac{\cos\theta}{r}\right], \tag{1.9}$$

where (1.7) is obtained from (1.4) using the constitutive relation and the definition of the curvatures is used to express κ_φ in terms of r and θ. In equations (1.8) and (1.9) t_s and t_φ are expressed in terms of α_s and α_φ through the scaled constitutive relations, and equation (1.8) is converted into a differential equation for α_s by eliminating α_φ through the relation $\alpha_\varphi = r/\rho$.

When bending moments can be neglected the shell no longer supports an out-of-plane shear force, *i.e.* $q_s = 0$. There is a corresponding simplification of the governing equations. In particular (1.9) reduces to $q_n/A = \kappa_s f_s + \kappa_\varphi f_\varphi$, which is just a generalized form of the Young-Laplace law. By casting this equation in dimensionless form one can easily identify a dimensionless parameter of the form $\xi = P_{\text{eff}} w/(hE)$ characterizing the overall deformation. Here w is a characteristic length scale (typically, the width of the tip) and P_{eff} is a measure of the normal stress acting on the walls. Detailed studies of the mechanical properties of microorganisms are difficult and only a few estimates have been proposed (See Table 1.)

Organisms	w	h	P	E	ξ	G	Ref
A. nidulans mature	3	46	1.4	115	0.8	0.2-0.5	Ma et al. ('05)
A. nidulans tip	3	46	1.4	75	1.2	0.2-0.5	Ma et al. ('05)
M. gryphiswaldenese	0.5	1	0.1	30	0.003		Thwaites ('89), Arnoldi ('00)

Table 1.1 w: width (μm), h: thickness (mm), P: Pressure (MPa), G: growth rate (μm/min), E: Young's modulus (MPa)

1.3 Modeling cell wall properties and growth

A fundamental component of any model of apical growth is the representation of the cell wall anisotropy. This will depend on the details of the cell wall architecture: for example, the degree of peptidoglycan cross-linking in actinomycetes, or the orientation of the cellulose microfibrils in root hairs [12]. Such biophysical detail is difficult to obtain experimentally and here we take a simpler phenomenological approach that captures the essence of the so called "soft-spot" hypothesis by prescribing the elastic response of the cell wall to vary along the meridional direction such that the distal regions of the hypha are practically rigid, while the regions near the tip have a much smaller elastic modulus corresponding to a softer material. At this level of modeling, a simple scaling argument shows that a softer material response can be interpreted as an increase in turgor pressure, and vice versa. This is the basis for the "effective pressure" model [5] and we continue to use it here. Thus we set $q_n^{(eff)} = Q/2\left[1 - \tanh\left(\frac{\sigma-\sigma_1}{a}\right)\right] + b$, where the parameter Q is given the

ratio of pressure to rigidity A at the tip and decays away from the tip as the rigidity increases. The parameters σ_1 and a describe the length of the apical extension zone. The parameter b describes the effective normal force far from the tip since $\lim_{\sigma\to\infty} q_n^{(eff)} = b$. In this region the cell walls are relatively rigid.

At the mathematical level, the process of growth is achieved by considering an evolving reference configuration parameterized by a time t. At any given time, the current configuration is obtained by loading the reference configuration with the turgor pressure P and computing the resulting shape for the given boundary conditions. The problem is then to describe the evolution of the reference configuration. The basic idea is that remodeling is achieved by assuming that it takes place so as to remove stresses present in the current configuration. Explicitly, we consider an *initial configuration* defined by the pair $(\sigma_0, \rho_0(\sigma_0))$ and a *reference configuration* defined by $(\sigma(\sigma_0,t), \rho(\sigma_0,t))$ with initial values $\sigma(\sigma_0,0) = \sigma_0$ and $\rho(\sigma_0,0) = \rho_0$. The deformation from the initial to the reference configuration is characterized by the *growth strains*

$$\gamma_s = \frac{d\sigma}{d\sigma_0}, \quad \gamma_\varphi = \frac{\rho}{\rho_0}. \tag{1.10}$$

The *current configuration* at a given time is defined by $(s(\sigma,t), r(\sigma,t))$ and is obtained by solving the mechanical problem of the shell under load, that is by computing the *elastic strains* from the reference configuration at time t to the current configuration at the same time t. Explicitly: $\alpha_s = ds/d\sigma, \alpha_\varphi = r/\rho$. Note that the mapping from the initial configuration to the current configuration is characterized by the product of the growth and elastic strains

$$\frac{ds}{d\sigma_0} = \alpha_s\gamma_s = \frac{ds}{d\sigma}\frac{d\sigma}{d\sigma_0}, \quad \frac{r}{\rho_0} = \alpha_\varphi\gamma_\varphi = \frac{r}{\rho}\frac{\rho}{\rho_0}. \tag{1.11}$$

That is, the growth and elastic processes are modeled through a multiplicative decomposition, similar to the one used in the theory of elastic growth [13] where the deformation tensor is decomposed into the product of two tensors, the growth tensor, mapping the initial configuration to an unstressed configuration and an elastic deformation tensor mapping the evolving reference configuration to the current configuration.

The introduction of the growth strains require a new constitutive relationships. Since they describe the evolution of the material in time, these relationships are usually referred to as *evolution laws* and take the form of differential equations for the growth rate relating the reference and current configurations at a time t to a new reference configuration at a time $t + dt$. If we assume that the remodeling process depend on the stress, these evolution laws take the general form

$$\frac{d\gamma_s}{dt} = \eta\mathscr{G}_s(\gamma_s, t_s, t_\varphi), \quad \frac{d\gamma_\varphi}{dt} = \eta\gamma_\varphi\mathscr{G}_\varphi(\gamma_s, t_s, t_\varphi). \tag{1.12}$$

where η^{-1} is a characteristic relaxation time, and $(\mathscr{G}_s, \mathscr{G}_\varphi)$ is a function of the stresses that vanishes at $(\gamma_s, t_s, t_\varphi) = (1,0,0)$.

In practice, the evolution laws are not known for microbial growth and we adopt a much simpler evolution rule by assuming that growth takes place so as to fully remove the stresses. That is we discretize the evolution law and assume that either the remodeling time is sufficiently fast or that the elastic deformation is sufficiently small so that at each time step the elastic stresses are fully relieved. We start with an initial shape defined by the function $\rho_0(\sigma_0)$, $0 \le \sigma_0 \le L_0$, and compute the new shape $r(\sigma_0)$ by solving the mechanical equations subject to the boundary condition $r(L_0) = R_0, r(0) = 0$. The new shape $r(\sigma_0)$ represents the new mechanical equilibrium of the membrane. Once the stresses are fully relieved, the new reference configuration is characterized by the pair $(\sigma_1 = s(\sigma_0, \rho_1(\sigma_1))$ which defines the new reference shape of length $L_1 = s(L_0)$ computed from equation (1.1). The new configuration is then used to compute a new mechanical equilibrium with boundary conditions $r(L_1) = R_0, r(0) = 0$ and so on.

1.4 Results

We begin by considering tip growth in the absence of surface stresses, *i.e.* $\tau_s = 0$. Using the membrane equations, a neo-Hookean energy, and an initially spherical shell with a soft spot, we can simulate the initial phases of hyphal growth a typical growth pattern over N time steps is shown in Figure 1.2. We also plot the corresponding values of the stresses (τ_s, τ_ϕ), and the deformation parameters $(\alpha_s, \alpha_\phi, \alpha_3)$. These plots support the hypothesis of maximal stress and strain in the vicinity of the apex. It is

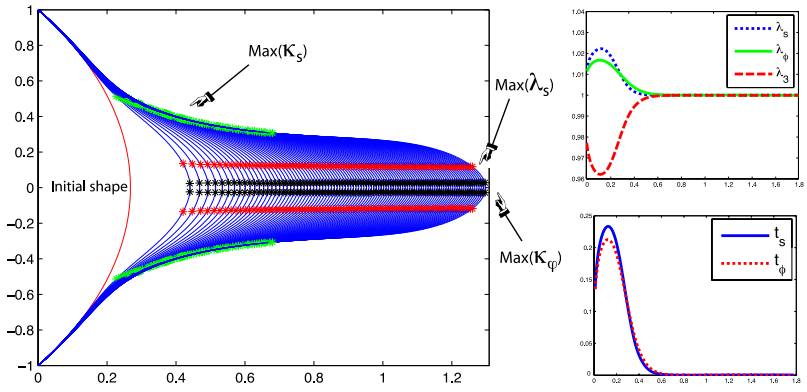

Fig. 1.2 (Left) Evolution of the tip in the absence of external surface stress. (Left panels) Profile of strains, and stresses at n=70 as a function of s ($\tau_s = 0$, $Q = 1$, $\sigma 1 = \pi/12$, $a = 1/8$, $b = 10^{-4}$).

interesting to note that the curvature of the tip is not maximal at the tip but close to the tip as observed in experiments [14].

A variety of numerical studies testing the effect of using different elastic energies such as the Mooney-Rivlin energy, and the effect of including bending moments,

did not reveal any significant changes to the above results. Accordingly we use the membrane equations and the neo-Hookean energy for the rest of our computations.

In many experiments, the tip propagation appears to be self-similar, namely that at each time step the newly grown tip looks like a translation of the tip shape at the previous instant. This suggests that in the course of apical growth dynamics it is this (temporal) self-similarity, which will depend delicately on the local environmental conditions and material parameters, that characterizes the propagation rather than a specific mathematical form of the tip shape. Here, we compute, over longer periods, the hyphal propagation for a number of different conditions. In each case we see the pattern long-time self-similarity (see Figure 1.3).

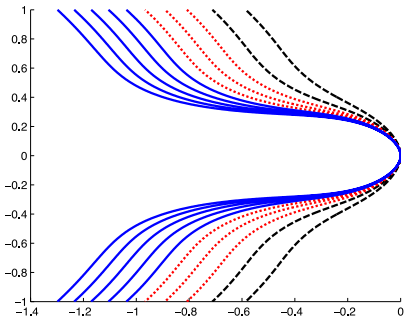

Fig. 1.3 Evolution of a tip shape seen in a reference frame moving with the tip. As growth proceeds, the shape converges towards a self-similar shape (growth proceeds from early growth (dashed curves), intermediate (dotted curves) to final (solid curves, curves are shown every 10 iterations (right to left)). (same parameters as previous figure).

1.5 Conclusion

The use of an exact elasticity formulation coupled with a simple representation of growth provides a mechanically self-consistent model that appears capable of of exploring and capturing many features of apical hyphal growth exhibited by a variety of different organisms. The formulation enables us to test the contributions of bending moments and the effects of various elastic energy functions on the hyphal expansion and indicates that the observed phenomena can be effectively captured with relatively simple elastic energies (such as the neo-Hookean or Mooney-Rivlin energy), and that bending moments do not play a significant role in determining the tip shape under typical growth conditions. The model also makes possible the inclusion of external tangential stresses corresponding to friction between the propagating tip and the surrounding medium [4]. The model captures a regime of self-similar tip propagation conditioned by the material properties of the cell wall and the local environment.

The model of growth used here is based on both a re-parameterization of the cell wall to take into account local wall buildup and a rigidification of the side wall due to remodeling. It is, implicitly, a stress-induced position-dependent evolution law. That is, growth occurs in regions of higher stresses but is also localized in an active region close to the tip. These two simple basic assumptions together with the possibility of elastic deformations determine the most important properties of tip growth observed experimentally, namely, a self-similar growth mechanisms in homogeneous conditions and a variety of tip shape depending on the elastic parameters, applied load, and remodeling behavior.

Acknowledgments: The authors would like to thank Prof. N. P. Money and J. Dumais for helpful discussions. This material is based in part upon work supported by the National Science Foundation under grant No. DMS-0604704 (A.G. and M. T.).

References

1. R. J. Howard. Ultrastructural analysis of hyphal tip cell growth in fungi: Spitzenkörper, cytoskeleton and endomembranes after freeze-substitution. *J. Cell. Science*, 48, 1981.
2. N. P. Money. Wishful thinking of turgor revisited: The mechanics of fungal growth. *Fungal Genetics and Biology*, 21, 1997.
3. S. Bartnicki-Garcia, C. E. Bracker, G. Gierz, R. Lopez-Franco, and H. S. Lu. Mapping the growth of fungal hyphae: Orthogonal cell wall expansion during tip growth and the role of turgor. *Biophys. J.*, 79(5):2382–2390, 2000.
4. A. Goriely and M. Tabor. Biomechanical modeling of growing filamentous cells. *Fungal Biology Reviews*, 22:77–83, 2008.
5. A. Goriely and M. Tabor. Biomechanical models of hyphal growth in actinomycetes. *J Theor Biol*, 222(2):211–218, 2003.
6. A. Goriely and M. Tabor. Self-similar tip growth in filamentary organisms. *Phys Rev Lett*, 90(10):108101, 2003.
7. E. A. Evans and R. Skalak. *Mechanics and thermodynamics of biomembranes*. CRC Press, Inc, Boca Raton, Florida, 1980.
8. R. S. Rivlin and D. W. Saunders. Large Elastic Deformations of Isotropic Materials. VII. Experiments on the Deformation of Rubber. *Philosophical Transactions of the Royal Society of London. Series A, Mathematical and Physical Sciences*, 243(865):251–288, 1951.
9. H. Ma, L. Snook, S. Kaminskyj, and T. Dahms. Surface ultrastructure and elasticity in growing tips and mature regions of aspergillus hyphae describe wall maturation. *Microbiology*, 151(Pt 11):3679–3688, 2005.
10. J. J. Thwaites and N. H. Mendelson. Mechanical properties of peptidoglycan as determined from bacterial thread. *Int. J. Biol. Macromol.*, 11(4):201–6, 1989.
11. M. Arnoldi, M. Fritz, E. Bauerlein, M. Radmacher, E. Sackmann, and A. Boulbitch. Bacterial turgor pressure can be measured by atomic force microscopy. *Phys. Rev. E.*, 62(1 Pt B):1034–1044, 2000.
12. J. Dumais, S. L. Shaw, C. R. Steele, S. R. Long, and P. M. Ray. An anisotropic-viscoplastic model of plant cell morphogenesis by tip growth. *Int. J. Develop. Biol.*, 50(2-3):209–222, 2006.
13. E. K. Rodriguez, A. Hoger, and McCulloch A. Stress-dependent finite growth in soft elastic tissue. *J. Biomechanics*, 27, 1994.
14. J. Dumais, S. R. Long, and S. L. Shaw. The Mechanics of Surface Expansion Anisotropy in Medicago truncatula Root Hairs. *Plant Physiology*, 136:3266–3275, 2004.